



Working standard gas saving system for in-situ CO₂ and CH₄ measurements and calculation method for concentrations and their uncertainty

Motoki Sasakawa¹, Noritsugu Tsuda², Toshinobu Machida¹, Mikhail Arshinov³, Denis Davydov³,
5 Aleksandr Fofonov³, Boris Belan³

¹Earth Science Division, Center for Global Environmental Research, National Institute for Environmental Studies, Tsukuba, 305-8506, Japan

²Global Environmental Forum, Tsukuba, 305-0061, Japan

³Institute of Atmospheric Optics, Russian Academy of Sciences, Siberian Branch, Tomsk, Russia

10 *Correspondence to:* Motoki Sasakawa (sasakawa.motoki@nies.go.jp)

Abstract. We have developed a container system for in-situ measurement of CO₂ and CH₄ that significantly reduces the consumption of working standard gases to a level less than one order of magnitude smaller than that required by a common method. It uses on-site compressed air to track the baseline drift of sensors. JR-STATION (Japan-Russia Siberian Tall Tower Inland Observation Network) consisted of this system installed at nine sites in Siberia. The system acquires semi-continuous data by recording several minutes of averaged data after gas replacement time. We have updated the calculation method for deriving CO₂ and CH₄ concentrations to determine their uncertainty for each data simultaneously. Furthermore, we estimated the system's reproducibility based on the repeated measurement of on-site compressed air. The CO₂ and CH₄ concentration reproducibility mostly varied by less than 0.2 ppm and five ppb, respectively. Uncertainties of time-averaged data were sometimes higher than the measurement uncertainty for each period, suggesting that the data include atmospheric variability during the measurement period of several minutes. Data users should consider the difference between the two uncertainties to select optimal data, depending on their focusing spatial scale. The CO₂ and CH₄ data measured with the NDIR and the tin dioxide sensor exhibited good agreement with those measured by the CRDS, respectively.

1 Introduction

It is known that accurate measurements of greenhouse gas concentrations require the analyzers to be calibrated against a set of standard gas mixtures. At least one of them (target) should be used hourly to track an NDIR (Non-Dispersive Infrared) analyzer's baseline drift (Andrews et al., 2014). A CRDS (Cavity Ring-Down Spectroscopy) analyzer is more stable and does not need frequent checks of the drift (ICOS RI, 2020). Delivering high-pressure cylinders to remote sites is a significant issue for long-term atmospheric monitoring. Thus, to reduce the consumption of gas, Watai et al. (2010) developed a system that utilizes on-site air as sub-working standard gas (SWS-gas) to track the baseline drift of the NDIR sensors. Watai et al. (2010)



30 then installed this system at a remote tower site at Berezorechka ($56^{\circ}08'45''\text{N}$ $84^{\circ}19'55''\text{E}$) in West Siberia in 2001 to measure CO_2 concentrations semi-continuously.

Concerning CH_4 measurement, a commonly used gas chromatograph with a flame ionization detector (GC/FID) requires hydrogen and carrier gases. It also needs significant power consumption. However, electric power is often restricted at remote sites. Thus, Suto and Inoue (2010) modified a tin dioxide sensor (TOS), which is widely used to detect natural gas leaks, to be
35 able to measure CH_4 in the atmosphere. The developed TOS unit does not need hydrogen and carrier gases. The nominal power consumption for the unit, consisting of TOS, temperature-stabilizer mechanism, and electronic circuits for the sensor and heater, is less than 10W.

We added the TOS unit to the system at the tower site in West Siberia, then expanded the tower observation network (Sasakawa et al., 2010; Sasakawa et al., 2012; Sasakawa et al., 2013). The tower network named JR-STATION (Japan-Russia Siberian
40 Tall Tower Inland Observation Network) now consists of six tower sites in West Siberia. Recently, we added CRDS analyzers at Karasevov ($58^{\circ}14'44''\text{N}$ $82^{\circ}25'28''\text{E}$) in 2015 (Picarro G2401), and at Demyanskoe ($59^{\circ}47'29''\text{N}$ $70^{\circ}52'16''\text{E}$) and Noyabrsk ($63^{\circ}25'45''\text{N}$ $75^{\circ}46'48''\text{E}$) in 2016 (Picarro G2301) to improve the robustness of the measurements. We have further updated the calculation method for calculating CO_2 and CH_4 concentrations to derive their uncertainty for each data simultaneously. Here, we describe the details of the modified measurement system and the calculation method. We also compare the data
45 produced with the NDIR (and the semiconductor sensor) and the CRDS data.

2 Method

2.1 Measurement system

Ambient air was taken from air sample inlets at two different heights (four at Berezorechka) on television and radio-relay communication towers (Table 1). Each sample inlet was mounted several meters away from the tower at the end of an extension
50 arm. The air from the inlets was sucked into the measurement system through the sampling lines (6-mm OD Decabon tube). The measurement system was housed in a freight container insulated to reduce temperature variation. A schematic diagram of the measurement system is shown in Fig. 1. The measurement system consists of a pump unit, a selector unit, and an analyzer unit. The pump unit was located upstream of the selector and analyzer unit to keep the downstream pressure higher than the ambient, which reduced the likelihood of bias in measurements due to any leak from many connections in the system. Two
55 diaphragm pumps (model N86KNE, KNF, Germany) delivered the sample air into the system. The sampling lines were flushed continuously with a flow rate of about seven standard liters per minute, and excess air was vented through the back-pressure valve ("BPV" in the pump unit). Then the air was dried by an adiabatic expansion in a glass water trap ("WT" in the pump unit) that was purged every hour via an NC solenoid valve, which was opened twice for 10 seconds to remove the condensed water. The sample air was also dried using a semipermeable membrane dryer (PD-625–24SS, Permapure, USA) ("Nafion" in
60 the selector unit) in the selector unit. The semipermeable membrane dryer removed water vapor from the pressurized inner tube to an outer tube where the split gas flowed (split sample method). The air from the upper and lower-level inlet, the three



working standard gases, and the sub-working standard gas (SWS-gas) were selected through a 6-port valve manifold. While the working standard gas or the SWS-gas flowed into the analyzer unit, the sample air was exhausted at the 6-port valve. In the analyzer unit, the sampled air was extra dried with magnesium perchlorate, which was fed into a stainless steel tube with a dimension of 2 cm in inner diameter and 10 cm in length (" $\text{Mg}(\text{ClO}_4)_2$ " in the analyzer unit). There were two tubes, and the flow path of the air switched from one to the other every month. The used magnesium perchlorate was replaced before the next run. After being dried with the magnesium perchlorate, the air retained its dewpoint at around $-50\text{ }^\circ\text{C}$ (39 ppm). The dehumidified air was then introduced into an NDIR analyzer (LI-820, LI-COR, USA; LI-7000 was used until September 2008 at BRZ) at a constant flow rate of 35 standard cubic centimeters per minute (sccm) set by a mass flow controller (SEC-E40, STEC, Japan). The CO_2 concentration was defined as the mole fraction in the dry air, and water vapor correction was not adopted. After passing through the NDIR, the air flowed into the TOS unit. A chemical desiccant made of P_2O_5 was installed in front of the TOS because it is necessary to keep water vapor below ten ppm in the sample air for this type of sensor. The sensor was designed to operate in areas lacking the sufficient infrastructure to sustain a conventional measurement system, such as a significant power source, carrier gas supply, and temperature-stabilized environment. The sensor has been verified against a gas chromatograph equipped with a flame ionization detector (Suto and Inoue, 2010). We additionally installed the CRDS (Picarro Inc.) analyzer at Karasevoe (G2401) in 2015, and at Demyanskoe and Noyabrsk (G2301) in 2016 to improve the system. The sampled air was split after leaving the 6-port valve, then fed into the CRDS at a constant flow rate of 35 sccm set by a mass flow controller (SEC-E40, STEC, Japan) through a semipermeable membrane dryer (model MD-050-72S-1, Permapure, USA). To protect the cavity of the CRDS from an inflow of the dissolved chemical desiccant ($\text{Mg}(\text{ClO}_4)_2$ or P_2O_5) in the accidental case of a broken pump etc., we equipped the CRDS with two poppet check valves ("PCV" in the analyzer unit).

Three working standard gases (STD1, STD2, STD3) were prepared from pure CO_2 and CH_4 diluted with purified air, and their concentrations were determined against the NIES 09 CO_2 scale (Machida et al., 2011) and NIES 94 CH_4 scale. Each scale was established by a series of standard gases prepared by the gravimetric method. Compared to the WMO- CO_2 -X2007 scale, the NIES 09 CO_2 scale is 0.09 ppm lower at a concentration of 376.2 ppm and 0.04 ppm lower at 404.91 ppm (Round Robin 6 Comparison Experiment). The NIES 94 CH_4 scale is 4.1 ppb higher than the WMO- CH_4 -X2004A scale at a concentration of 1736.3 ppb and 5.5 ppb higher at 1941.9 ppb (Round Robin 6 Comparison Experiment).

Table 1. Main features of the towers in the network of tall towers used for continuous long-term atmospheric CO_2 and CH_4 measurements over Siberia.

Identifying Code	Location	Latitude	Longitude	Air inlet heights (m)	Elevation at tower base (m a.s.l) ¹
BRZ	Berezorechka	56°08'45"	84°19'55"	5, 20, 40, 80	168
KRS	Karasevoe	58°14'44"	82°25'28"	35, 67	76



IGR	Igrim	63°11'30"	64°24'50"	24, 47	9
NOY	Noyabrsk	63°25'45"	75°46'48"	21, 43	108
DEM	Demyanskoe	59°47'29"	70°52'16"	45, 63	63
SVV	Savvushka	51°19'31"	82°07'42"	27, 52	495
AZV	Azovo	54°42'18"	73°01'45"	29, 50	110
VGN	Vaganovo	54°29'50"	62°19'29"	42, 85	192
YAK	Yakutsk	62°05'19"	129°21'21"	11, 77	264

¹Approximate estimates from Google earth.

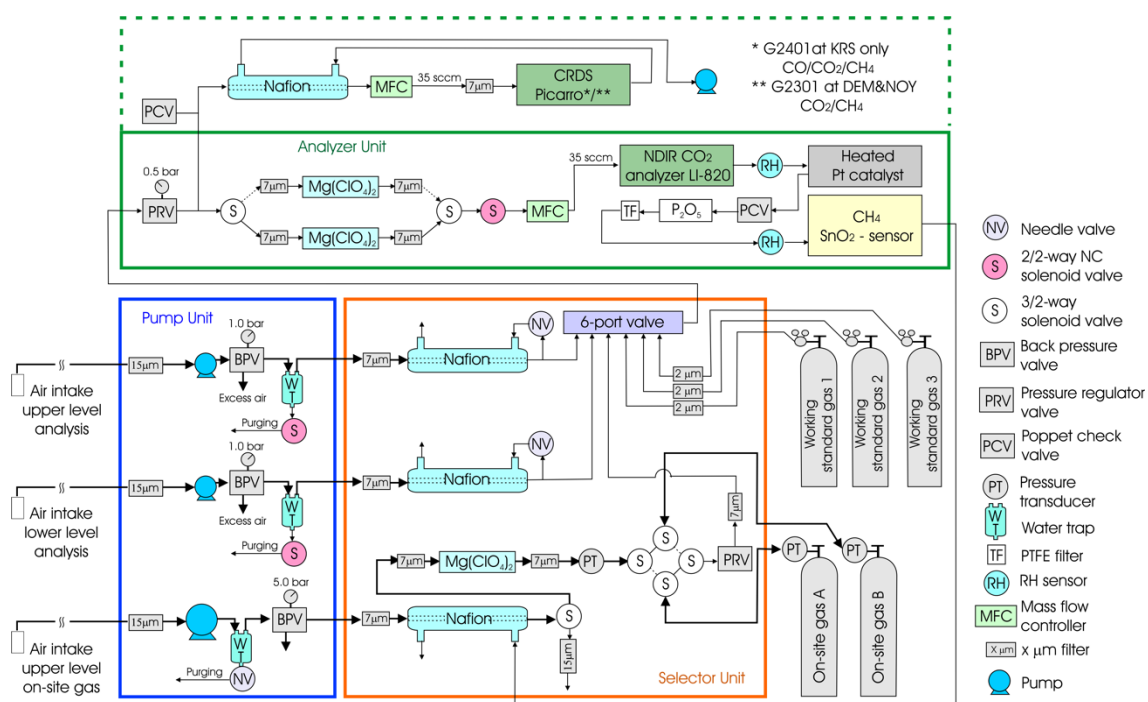


Figure 1. Schematic diagram of tower observation system.

95

A frequent calibration with working standard gases within 1-2 hours is necessary to conduct precise measurements of CO₂ and CH₄ because the output of the NDIR analyzer or the TOS could vary depending on the environment (atmospheric pressure etc.) in 1-2 hours. But if the calibration were done at this frequency, standard gases would be consumed in less than a year. Because delivering working standard gases to remote sites is a significant issue, we utilized on-site compressed air as SWS-
 100 gas to track the sensors' baseline drift, which reduced the consumption of the three standard gases. The on-site compressed air ("On-site gas A/B" in Fig. 1) was analyzed every hour, and the working standard gases were measured every 12 hours to calibrate the span of the sensors (details of the sequence are shown below). To prepare the SWS-gas, air from the highest inlet



was compressed by a pump (LOA-P103-NO, GAST, USA) into an aluminum cylinder (0.048 m³) for about 5 hours to approximately 0.35 MPa, after having been passed through a similar triple dehumidification path as the sampled air (a stainless steel water trap, a semipermeable membrane dryer (SWF- M06-400, AGC, Japan), and magnesium perchlorate). Two cylinders were prepared for the SWS-gas; one for compression and preservation and the other for the hourly measurements. The cylinders were automatically exchanged when the inner pressure in one used for measurements decreased below 0.1 MPa, which generally took about one week.

Air temperature and relative humidity were measured at both heights on the tower using commercial sensors (HMP45D, Vaisala, Finland). A wind monitor (model 81000, R. M. Young, USA) determined wind direction and speed at the higher inlet. Solar radiation was measured by a pyranometer (CM3, Kipp & Zonen, Netherlands), and precipitation by a tipping bucket rain gauge (model 52202, R. M. Young, USA) on the top of the container laboratory.

The analysis operation and data logging were performed by a measurement and control system (CR10X datalogger, CAMPBELL, USA). Stored data were retrieved once a month when both a system check and replacement of consumables (e.g., chemical desiccants) took place.

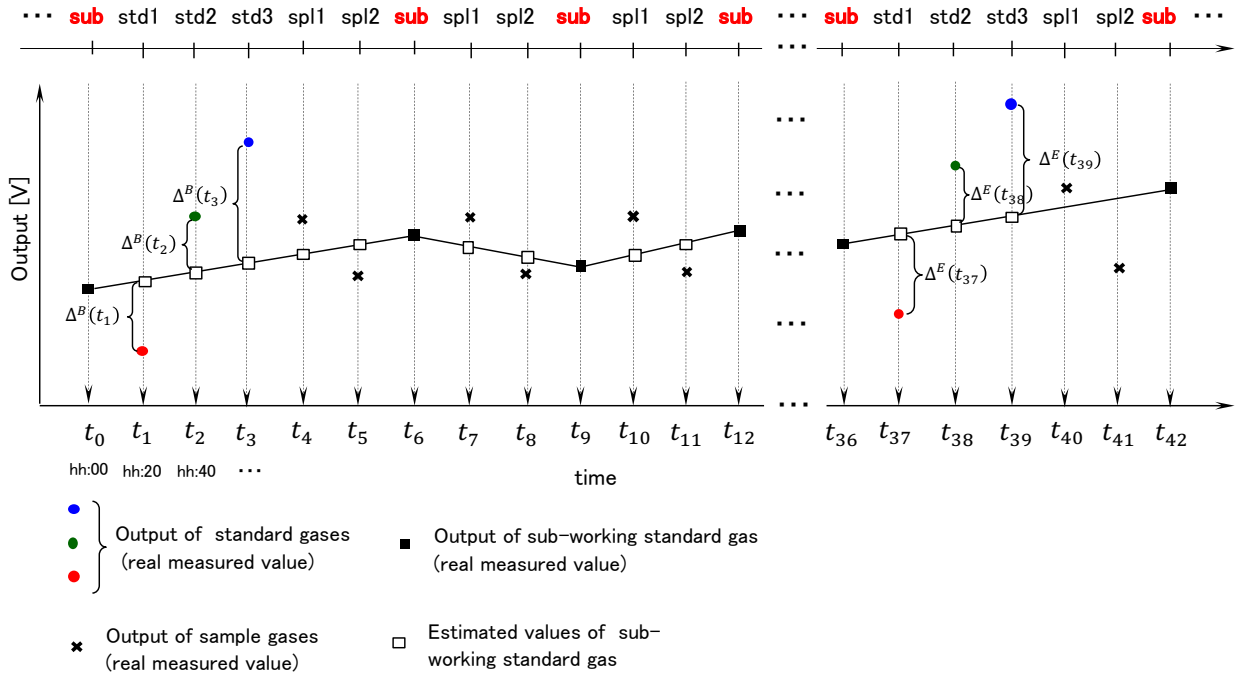
2.2 Measurement sequence

To be able to measure air at two heights, the air-sampling flow path was rotated every 20 min with the 6-port valve in the selector unit; that is, the higher inlet was sampled from hh:00 to hh:20, the lower inlet from hh:20 to hh:40, and the SWS-gas from hh:40 to (hh+1):00. During the first 17 min of each 20-min sampling interval, the system is flushing to equilibrate the air sample after switching. The final three-minute readouts were averaged and reported as the representative output data for the applicable one-hour period. Measurement frequency was 3 sec; thus, only the average and standard deviation of 60 readouts in voltage were stored in the CR10X. This was to minimize the data size for the limited storage capacity. The timestamp was the end time of every 20-min measurement interval. To exclude unreliable data, sometimes resulting from the system malfunction, the data was not used for sample calculation when the average data for the SWS-gas or working standard gases, which show essentially slight fluctuation, had a more significant standard deviation than a determined threshold (2 mV for CO₂, 5 mV for CH₄). Furthermore, we did not calculate the concentration of the sample when the outputs of the adjacent SWS-gas measurements varied largely. The raw data collected with the CRDS analyzer were stored in the CRDS' hard disk and processed after downloading in our laboratory.

Figure 2 shows the schematic measurement sequence for half a day. In the Fig. 2, we defined when the SWS-gas was measured just before an arbitrary series of working standard gas measurements as t_0 . Then we numbered the time of the following measurements in turn. We also defined the series of standard gas measurements at the beginning of the 12 hours as “B” and at the end as “E”.



std1-3 : Standard gas1-3
 spl1-2 : Sample gas (1=High altitude , 2=Low altitude)
 sub : Sub-working standard gas



135

Figure 2. Measurement sequence for a half day between subsequent measurements of working standard gases.

2.3 Quality check of the standard gas measurements

140 First, we checked the relationship among three standard gas measurements. We calculated the differences ($\Delta^B(t_i)$, $\Delta^E(t_j)$) between the measured output voltages of the standard gases ($V_{std}(t_i)$, $V_{std}(t_j)$) and the estimated one of the SWS-gas at the time of the standard gas measurement (Fig. 2). Here $i = 1, 2, 3$, and $j = 37, 38, 39$. The output value of the SWS-gas was interpolated by time using the closest output of the SWS-gas before and after the series of standard gas measurements. Thus, these values and their variances are expressed as:

$$\Delta^B(t_i) = V_{std}(t_i) - \left(\frac{6-i}{6} \cdot V_{sub}(t_0) + \frac{i}{6} \cdot V_{sub}(t_6) \right) \quad (1)$$

$$145 \quad (\sigma^B(t_i))^2 = (\sigma_{std}(t_i))^2 + \left(\frac{6-i}{6} \cdot \sigma_{sub}(t_0) \right)^2 + \left(\frac{i}{6} \cdot \sigma_{sub}(t_6) \right)^2 \quad (2)$$

$$\Delta^E(t_j) = V_{std}(t_j) - \left(\frac{42-j}{6} \cdot V_{sub}(t_{36}) + \frac{j-36}{6} \cdot V_{sub}(t_{42}) \right) \quad (3)$$

$$(\sigma^E(t_j))^2 = (\sigma_{std}(t_j))^2 + \left(\frac{42-j}{6} \cdot \sigma_{sub}(t_{36}) \right)^2 + \left(\frac{j-36}{6} \cdot \sigma_{sub}(t_{42}) \right)^2 \quad (4)$$



We estimated the output of STD1 at t_2 by adding $\Delta^B(t_1)$ to the estimated one of the SWS-gas at t_2 . We also evaluated the output of STD3 at t_2 by adding $\Delta^E(t_3)$ to the estimated one of the SWS-gas at t_2 . The same estimation was done at t_{38} . We then made
150 a linear calibration line with the output of STD2 and the estimated outputs of STD1 and STD3. Only those sets of the three standard gas measurements whose coefficients of determination were higher than 0.999 for CO₂ and 0.99 for CH₄ were adopted for the following calculation.

The difference in output (voltage) between Δ^B and Δ^E for each standard gas was defined as follows:

$$\delta_{(1,37)} = \Delta^E(t_1) - \Delta^B(t_{37}) \quad (5)$$

$$155 \quad \delta_{(2,38)} = \Delta^E(t_2) - \Delta^B(t_{38}) \quad (6)$$

$$\delta_{(3,39)} = \Delta^E(t_3) - \Delta^B(t_{39}) \quad (7)$$

The δ must be small unless the system is unstable, e.g., when the sensitivity of the sensors changes considerably for some reason. To exclude the data obtained during system malfunction, we determined a threshold for δ by converting it into concentration (<5.0 ppm for CO₂, <50 ppb for CH₄). Data showing values over the threshold were excluded from the
160 calculation. The difference in CO₂ concentration between sides B and E was calculated as follows:

$$\overline{\delta_{(i,j)}^B} = |\delta_{(i,j)} / S^B| \quad (8)$$

$$\overline{\delta_{(i,j)}^E} = |\delta_{(i,j)} / S^E| \quad (9)$$

where S^B and S^E are the slopes of the linear regression line at sides B and E . Because the x-axis of the calibration line for CH₄ is the logarithm of the concentration, the difference in CH₄ concentrations was calculated as:

$$165 \quad \overline{\delta_{(i,j)}^B} = C_i \cdot \left| e^{\frac{\delta_{(i,j)}}{S^B}} - 1 \right| \quad (10)$$

$$\overline{\delta_{(i,j)}^E} = C_i \cdot \left| e^{-\frac{\delta_{(i,j)}}{S^E}} - 1 \right| \quad (11)$$

where C_i is the concentration of the standard gas.

2.4 Calculation of the sample concentration and its uncertainty

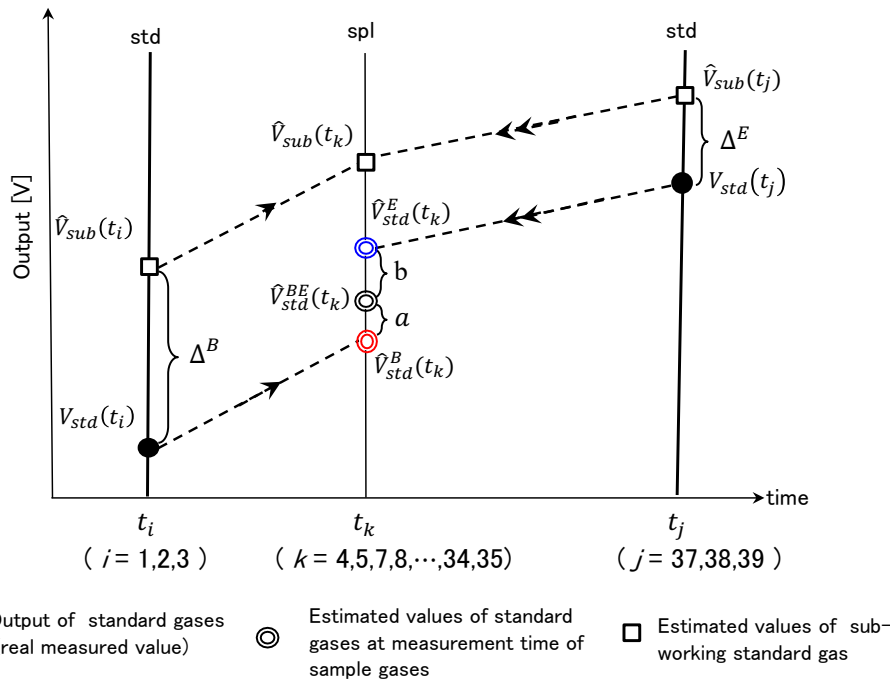
170 The analysis precision for this system was uniformly estimated as 0.3 ppm for CO₂ (Watai et al., 2010). Concerning CH₄ precision, Sasakawa et al. (2010) estimated it as 3.0 ppb based on the result of Suto and Inoue (2010). However, the experiment condition by Suto and Inoue (2010) was different from the gas-saving system. Instead, they connected only the working standard gases to the TOS, then reported the standard deviation of repeated measurements. The CH₄ analysis precision for this system thus could be more significant than 3.0 ppb. Furthermore, the sensitivity and stability of the sensor could differ
175 depending on the individual sensor and the condition of the individual system. We thus have updated the method for calculating the CO₂ and CH₄ concentrations to derive their uncertainty for each data simultaneously.



2.4.1 Estimation of the output values of working standard gases and their uncertainty at the time of the air sample measurements

180 We estimated the outputs in voltage of three standard gases at each measurement time of the sample air by interpolating the outputs of the three working standard gases depending on the difference of the outputs in voltage of the SWS-gas only between both standard gases satisfied the criteria described in section 2.3. Depending on the time difference between the targeted sample (t_k ; $k = 4, 5, 7, 8, \dots, 34, 35$) and standard gases at both sides B and E ((t_i, t_j) ; $(i, j) = (1, 37), (2, 38), (3, 39)$), the representative value ($\hat{V}_{std(t_i, t_j)}^{BE}(t_k)$) and its variance ($(\hat{\sigma}_{std(t_i, t_j)}^{BE}(t_k))^2$) were estimated as follows (Fig. 3):

std: Standard gas spl: Sample gas



185

Figure 3. Schematic diagram of the estimation method for the output of the standard gas at the time of sample air measurement.

$$\begin{aligned} \hat{V}_{std(t_i, t_j)}^{BE}(t_k) &= \frac{a}{a+b} \cdot \hat{V}_{std(t_i)}^B(t_k) + \frac{b}{a+b} \cdot \hat{V}_{std(t_j)}^E(t_k) \\ &= \hat{V}_{sub}(t_k) + \frac{1}{a+b} \cdot \{ a \cdot \Delta^B(t_i) + b \cdot \Delta^E(t_j) \} \end{aligned} \quad (12)$$

$$\begin{aligned} 190 \quad \left(\hat{\sigma}_{std(t_i, t_j)}^{BE}(t_k) \right)^2 &= \left(\hat{\sigma}_{sub}(t_k) \right)^2 + \left(\frac{a}{a+b} \cdot \sigma_{std}(t_i) \right)^2 + \left(\frac{a}{a+b} \cdot \frac{6-i}{6} \cdot \sigma_{sub}(t_0) \right)^2 \\ &+ \left(\frac{a}{a+b} \cdot \frac{i}{6} \cdot \sigma_{sub}(t_6) \right)^2 + \left(\frac{b}{a+b} \cdot \sigma_{std}(t_j) \right)^2 + \left(\frac{b}{a+b} \cdot \frac{42-j}{6} \cdot \sigma_{sub}(t_{36}) \right)^2 \end{aligned}$$



$$+ \left(\frac{b}{a+b} \cdot \frac{j-36}{6} \cdot \sigma_{sub}(t_{42}) \right)^2 \quad (13)$$

where $a : b = (t_j - t_k) : (t_k - t_i)$. Hat “^” means estimated value. $\hat{V}_{sub}(t_k)$ was calculated by interpolating the output of the SWS-gas value nearest to the targeted sample as follows:

195 {spl1 | $k = 4$ }

$$\hat{V}_{sub}(t_4) = \frac{1}{3} \cdot V_{sub}(t_0) + \frac{2}{3} \cdot V_{sub}(t_6) \quad (14)$$

{spl1 | $k = 7, 10, 13, \dots, 34$ }

$$\hat{V}_{sub}(t_k) = \frac{2}{3} \cdot V_{sub}(t_{k-1}) + \frac{1}{3} \cdot V_{sub}(t_{k+2}) \quad (15)$$

{spl2 | $k = 5$ }

200 $\hat{V}_{sub}(t_5) = \frac{1}{6} \cdot V_{sub}(t_0) + \frac{5}{6} \cdot V_{sub}(t_6)$ (16)

{spl2 | $k = 8, 11, 14, \dots, 35$ }

$$\hat{V}_{sub}(t_k) = \frac{1}{3} \cdot V_{sub}(t_{k-2}) + \frac{2}{3} \cdot V_{sub}(t_{k+1}) \quad (17)$$

Here $V_{sub}(t_l)$ {sub | $l = 0, 6, 9, 12, \dots, 36$ } is the measured value. In the following, a calculation example of $\hat{V}_{std}^{BE}(t_i, t_j)(t_k)$ and the variance for the case {spl1 | $k = 4, (i, j)$ } are given without any estimated value.

205 {spl1 | $k = 4, (i, j) = (1, 37), (2, 38), (3, 39)$ }

$$\begin{aligned} \hat{V}_{std}^{BE}(t_i, t_j)(t_4) &= \frac{1}{3} \cdot V_{sub}(t_0) + \frac{2}{3} \cdot V_{sub}(t_6) + \frac{a}{a+b} \cdot \left\{ V_{std}(t_i) - \left(\frac{6-i}{6} \cdot V_{sub}(t_0) + \frac{i}{6} \cdot V_{sub}(t_6) \right) \right\} \\ &+ \frac{b}{a+b} \cdot \left\{ V_{std}(t_j) - \left(\frac{42-j}{6} \cdot V_{sub}(t_{36}) + \frac{j-36}{6} \cdot V_{sub}(t_{42}) \right) \right\} \end{aligned} \quad (18)$$

$$\left(\hat{\sigma}_{std}^{BE}(t_i, t_j)(t_4) \right)^2 = \left(\frac{1}{3} \cdot \sigma_{sub}(t_0) \right)^2 + \left(\frac{2}{3} \cdot \sigma_{sub}(t_6) \right)^2$$

$$+ \left(\frac{a}{a+b} \cdot \sigma_{std}(t_i) \right)^2 + \left(\frac{a}{a+b} \cdot \frac{6-i}{6} \cdot \sigma_{sub}(t_0) \right)^2 + \left(\frac{a}{a+b} \cdot \frac{i}{6} \cdot \sigma_{sub}(t_6) \right)^2$$

210 $+ \left(\frac{b}{a+b} \cdot \sigma_{std}(t_j) \right)^2 + \left(\frac{b}{a+b} \cdot \frac{42-j}{6} \cdot \sigma_{sub}(t_{36}) \right)^2 + \left(\frac{b}{a+b} \cdot \frac{j-36}{6} \cdot \sigma_{sub}(t_{42}) \right)^2$ (19)

2.4.2 Estimation of sample air concentration and estimation uncertainty using a calibration line

We calculated a calibration line with the estimated outputs of standard gases ($\hat{V}_{std}^{BE}(t_i, t_j)(t_k)$) and their variances

($\left(\hat{\sigma}_{std}^{BE}(t_i, t_j)(t_k) \right)^2$) at the time of the sample measurement obtained in the section 2.4.1. A linear line ($y = Sx + I$; y : output

215 in voltage, x : concentration for CO₂ and log(concentration) for CH₄) was adopted for the calibration line (Fig. 4).

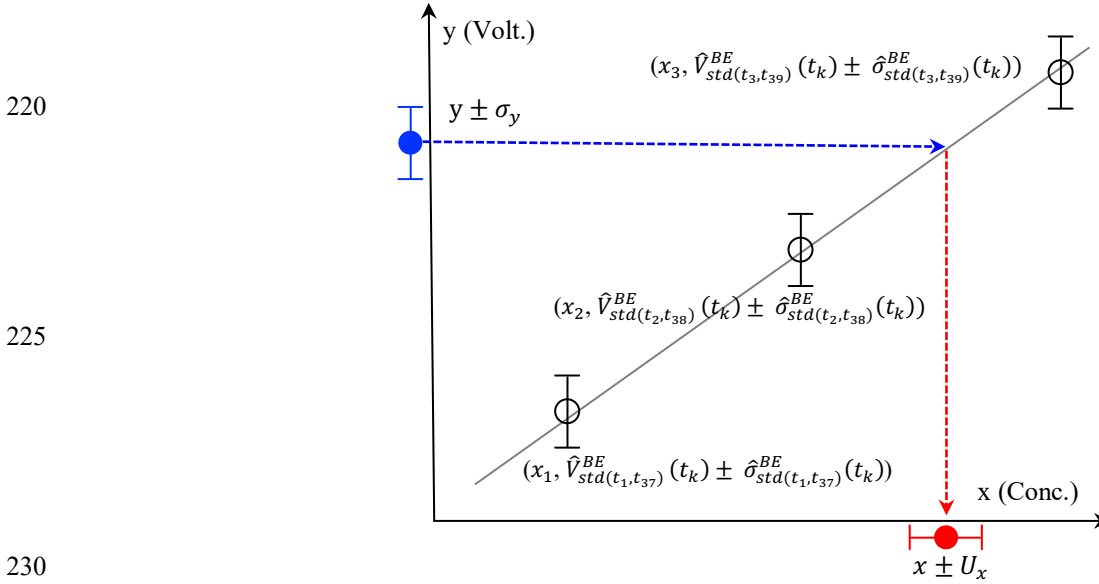


Figure 4. Schematic diagram for estimating the CO₂ and CH₄ concentration (x) of the gases and estimation uncertainty (U_x) from the output in voltage (y) with its standard deviation (σ_y). The gray line indicates the estimated linear calibration line ($y = Sx + I$).

Following the likelihood method, we identified the slope (S) and intercept (I) for every sample time (k) at the maximum of the

likelihood function (L). Solving the normal equation of $\begin{cases} \frac{\partial L}{\partial S} = 0 \\ \frac{\partial L}{\partial I} = 0 \end{cases}$, S and I were obtained as follows:

$$S(k) = \frac{(\sum w_{ijk})(\sum w_{ijk}x_i y_{ijk}) - (\sum w_{ijk}x_i)(\sum w_{ijk}y_{ijk})}{(\sum w_{ijk})(\sum w_{ijk}x_i^2) - (\sum w_{ijk}x_i)^2} \quad (20)$$

$$I(k) = \frac{(\sum w_{ijk}y_{ijk})(\sum w_{ijk}x_i^2) - (\sum w_{ijk}x_i y_{ijk})(\sum w_{ijk}x_i)}{(\sum w_{ijk})(\sum w_{ijk}x_i^2) - (\sum w_{ijk}x_i)^2} \quad (21)$$

where x_i is working standard gas concentration determined against the NIES scale. y_{ijk} is the estimated outputs of standard gas

($\hat{V}_{std(t_i, t_j)}^{BE}(t_k)$) and w_{ijk} is the reciprocal of the variance ($1/(\hat{\sigma}_{std(t_i, t_j)}^{BE}(t_k))^2$). Σ indicates the sum of i (three standard gases)

and the same for the following discussion. As shown in Section 2.4.1, the combinations of (i, j) are (1, 37), (2, 38), and (3, 39).

We omitted i, j , and k for the following expression. The inverse function was used because we estimated the concentration from the output in voltage. Furthermore, because the calibration line passes through the weighted mean point $(\bar{x}, \bar{y}) =$

$(\frac{\sum wx}{\sum w}, \frac{\sum wy}{\sum w})$, we practically used the following line:

$$x = \frac{y - \bar{y}}{S} + \bar{x} \quad (22)$$

The uncertainty for the estimated concentration (x) was calculated with the following equation:



$$U_x^2 = \left(\frac{\partial x}{\partial y}\right)^2 U^2(y) + \left(\frac{\partial x}{\partial \bar{y}}\right)^2 U^2(\bar{y}) + \left(\frac{\partial x}{\partial S}\right)^2 U^2(S) + \left(\frac{\partial x}{\partial \bar{x}}\right)^2 U^2(\bar{x}) \quad (23-1)$$

where U is uncertainty for each component. The first term expresses the contribution from the variation in output of the measured air (σ_y) and 60 repeated measurements:

$$\left(\frac{\partial x}{\partial y}\right)^2 U^2(y) = \frac{\sigma_y^2}{S^2} \cdot \frac{1}{60}$$

250 The second term expresses the contribution from the variation in \bar{y} :

$$\left(\frac{\partial x}{\partial \bar{y}}\right)^2 U^2(\bar{y}) = \frac{1}{S^2} \frac{\sum w^2 \sigma^2}{(\sum w)^2} = \frac{1}{S^2} \cdot \frac{1}{\sum w}$$

where σ^2 is the variance of the output for standard gases constituting the calibration line. The third term expresses the contribution from the variation in the slope of the calibration line (S):

$$\left(\frac{\partial x}{\partial S}\right)^2 U^2(S) = \frac{\left(y - \frac{\sum wy}{\sum w}\right)^2}{S^4} \cdot \sum \sigma^2 \left(\frac{\partial S}{\partial y}\right)^2 = \frac{\left(y - \frac{\sum wy}{\sum w}\right)^2}{S^4} \cdot \frac{\sum w}{(\sum w)(\sum wx^2) - (\sum wx)^2}$$

255 The fourth term expresses the contribution from the variation in \bar{x} . In most cases, the uncertainty for the concentration of standard gases is not given, or it can be negligible compared with other uncertainties. Thus, we neglected this term. Summarizing all the terms, the uncertainty for the estimated concentration (x) is as follows:

$$U_x = \frac{1}{S} \cdot \sqrt{\frac{\sigma_y^2}{60} + \frac{1}{\sum w} + \frac{1}{S^2} \cdot \frac{(\sum w)y - \sum wy}{(\sum w)^2(\sum wx^2) - (\sum w)(\sum wx)^2}} \quad (23-2)$$

260 Since the calculation was done for the logarithm of the concentration for CH₄, the uncertainty for the estimated concentration was determined differently for the higher level ($U^+ = x(e^{U_x} - 1)$) and lower level ($U^- = x(1 - e^{-U_x})$). However, the average value is expressed as the uncertainty since the difference is less than 0.1 ppb in real terms.

2.4.3 Reproducibility check with the SWS-gas measurement

265 We calculated a calibration line only when the SWS-gas measurements closest to both sides of the sample measurements were normal. The normality of the SWS-gas measurement was assessed as follows. The same on-site compressed air was measured several times (for about a week) since the air was used as SWS-gas until its pressure dropped below 0.1 MPa. The on-site compressed air output value would vary smoothly if the system were stable. However, a gap would appear if the system temporarily became unstable. To detect any gap, we first estimated the output of standard gases at the time of the target SWS-gas measurement by interpolating $\Delta^B(t_i)$ and $\Delta^E(t_j)$ based on the output value of the target SWS-gas itself (section 2.4.1).

270 Then, calculating a calibration line with the estimated output of standard gases, we obtained the concentration of the target SWS-gas. Second, we estimated the output value of the SWS-gas at the time of the target SWS-gas measurement by interpolating the outputs of the two adjacent SWS-gases. Then, we determined the concentration of the target SWS-gas in the same manner. If these estimated concentrations differed from each other by more than one ppm for CO₂ and ten ppb for CH₄,



we regarded the target SWS-gas data as abnormal. This assessment was done while the adjacent SWS-gas measurements were
275 conducted for the same on-site compressed air.

We then checked the system's stability with the measurement of the SWS-gas. Interpolating the outputs of the SWS-gases
adjacent to the standard gas measurements, we calculated the concentrations of the SWS-gas with the calibration line at the
time of STD2, which was used to assess the coefficient of determination in Section 2.3. We regarded the estimated
concentrations of the SWS-gas as independent; thus, we obtained 14 estimated concentrations if the measurements for the
280 same SWS-gas continued for a week. We determined a threshold for the standard deviation (σ_{SWS} ; 1 ppm for CO₂, 10 ppb for
CH₄) and the fluctuation range (5 ppm for CO₂ and 20 ppb for CH₄) obtained from the estimated independent data set. All the
data that exceeded the threshold were deleted.

The standard deviation of the remaining stable data provides reproducibility of repeat measurements every 12 hours for a given
period (often a week). From the point of this procedure, the SWS-gas equates with the 'target tank' or 'surveillance tank'
285 mentioned in the GAW report (WMO, 2018). Regardless of the site or time of measurement, σ_{SWS} for CO₂ mostly was below
0.2 ppm, and for CH₄ was below five ppb (As examples, NOY data are shown in Supplement Fig. S1-S6). Note that the
standard deviation of the output (σ_y) of the sample air could become significant due to large diurnal variation during summer
since the output of the sample air could include a natural variation of the atmosphere during the measurement period of three
minutes. As a result, the uncertainty obtained for each sample air concentration (U_{x_sample}) with equation 23-2 could be more
290 considerable than the reproducibility (σ_{SWS}). GAW report (WMO, 2018) mentioned that both values should be reported, and
 U_{x_sample} provides a quantitative indicator of the influence of nearby sources and can be used for data selection and weighting
in applications such as inverse modeling. Following this guide, we showed U_{x_sample} and σ_{SWS} in our data set. A flow chart for
the calculation method is shown in Fig. 5.

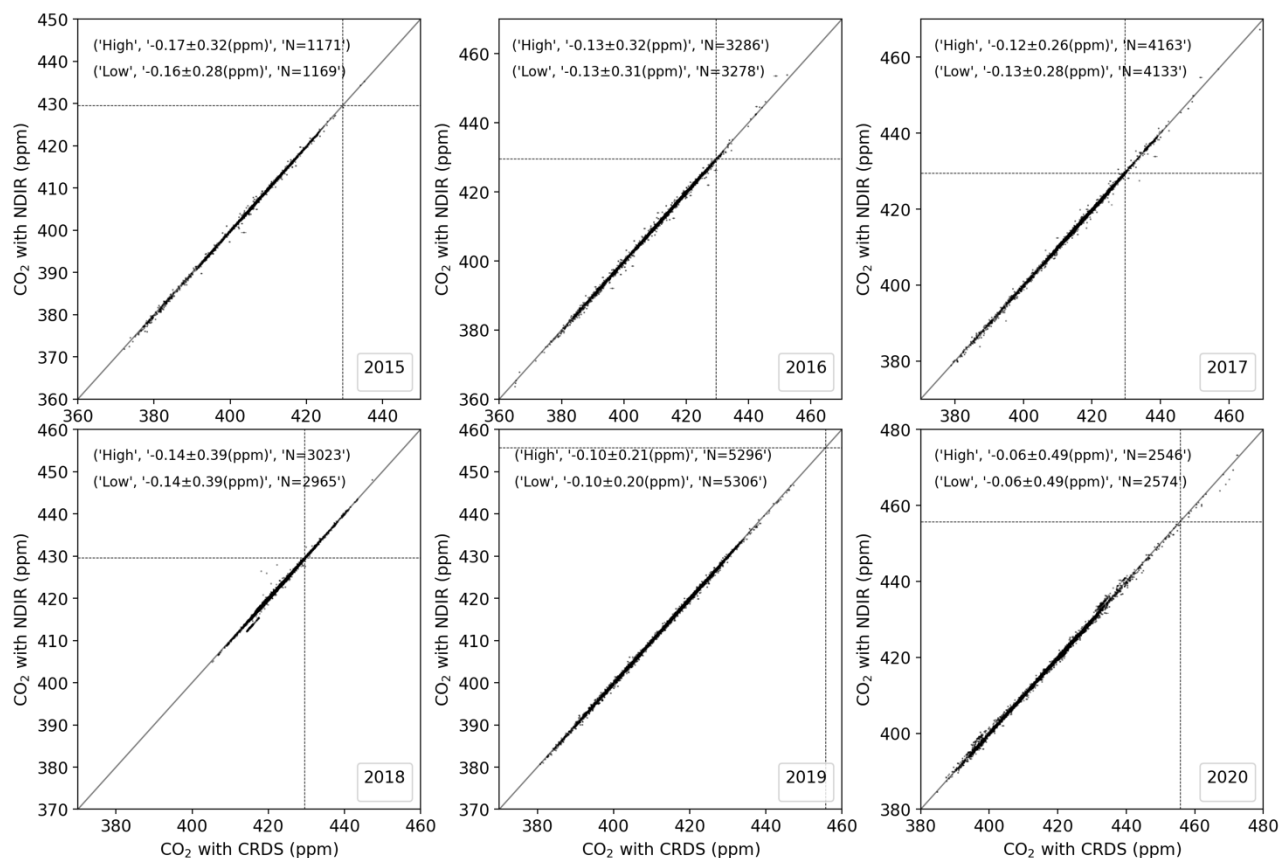


295 Figure 5. Flow chart of concentration calculation method.



2.5 Comparison between NDIR/TOS and CRDS

The CRDS was installed at KRS in July 2015, DEM in June 2016, and NOY in August 2016. The CRDS is a highly stable analyzer used in greenhouse gas observations worldwide (Kwok et al., 2015). We compared the recalculated NDIR (and
300 semiconductor sensor) values with the CRDS values (Fig. 6, Fig. 7, Supplement Fig. S7-S10). The flow path branches off after the 6-port valve (Fig. 1), so the same air is analyzed. The CRDS operates independently of the existing system, so information on instrument error flags and valve switching timing is not linked to the measured data. Therefore, by detecting the CH₄ concentration of the lowest standard gas, the timing of the standard gas measurement was captured and timed. Only data from the period when the system was normal was extracted. The CRDS output values were converted to the NIES scale and averaged
305 over three minutes for comparison. The temperature in the CRDS (data column name is 'WarmBoxTemperature') was kept constant (45.00°C). Still, it rarely changed by more than 0.02°C in 3 minutes in DEM and NOY, and the CO₂ concentration fluctuated more in such cases. The CH₄ concentration, on the other hand, was not affected by this temperature change. Since some observed values exceeded the highest concentration of the standard gas, only values within the concentration range of the standard gas were used to calculate the difference between the two. There was no significant difference in CO₂
310 concentration regardless of the inlet at both altitudes. No significant difference was found for CH₄ concentration either. However, the difference in NOY was highly variable, and the TOS values tended to be significantly higher. The sensor is also sensitive to CO and H₂ in the air, so these gases are removed by installing a catalyst just before the sensor. However, it was found that the catalyst had deteriorated, and a new catalytic unit had to be added. The sensitivity of CO and H₂ to the semiconductor sensor is reported to be about 10% of that by CH₄ (Suto and Inoue, 2010), but if CO (about 100 ppb) and H₂
315 (about 500 ppb) are not removed at all from the air, an excess of about 60 ppb as CH₄ concentration could be detected. In NOY, it is expected that the temperature regulation of the catalytic unit did not work well and the catalyst did not function; only the CRDS measurements of the CH₄ concentration in NOY shall be used.



320 **Figure 6. Relationship between CO₂ concentration measured by the NDIR and the CRDS during ambient air measurements at KRS. The CRDS 3-minute measurements are averaged on the horizontal axis, and the NDIR values are on the vertical axis. Error bars on the horizontal axis are the standard error of the averaged data. Error bars on the vertical axis are U_{x_sample} . The gray line represents the 1:1 line. The dotted lines indicate the highest concentration of standard gases. The average difference between NDIR and CRDS (NDIR – CRDS) for each inlet is represented in the figure (mean ± SD). Only data that were within the standard gas concentration**

325 **range were used.**

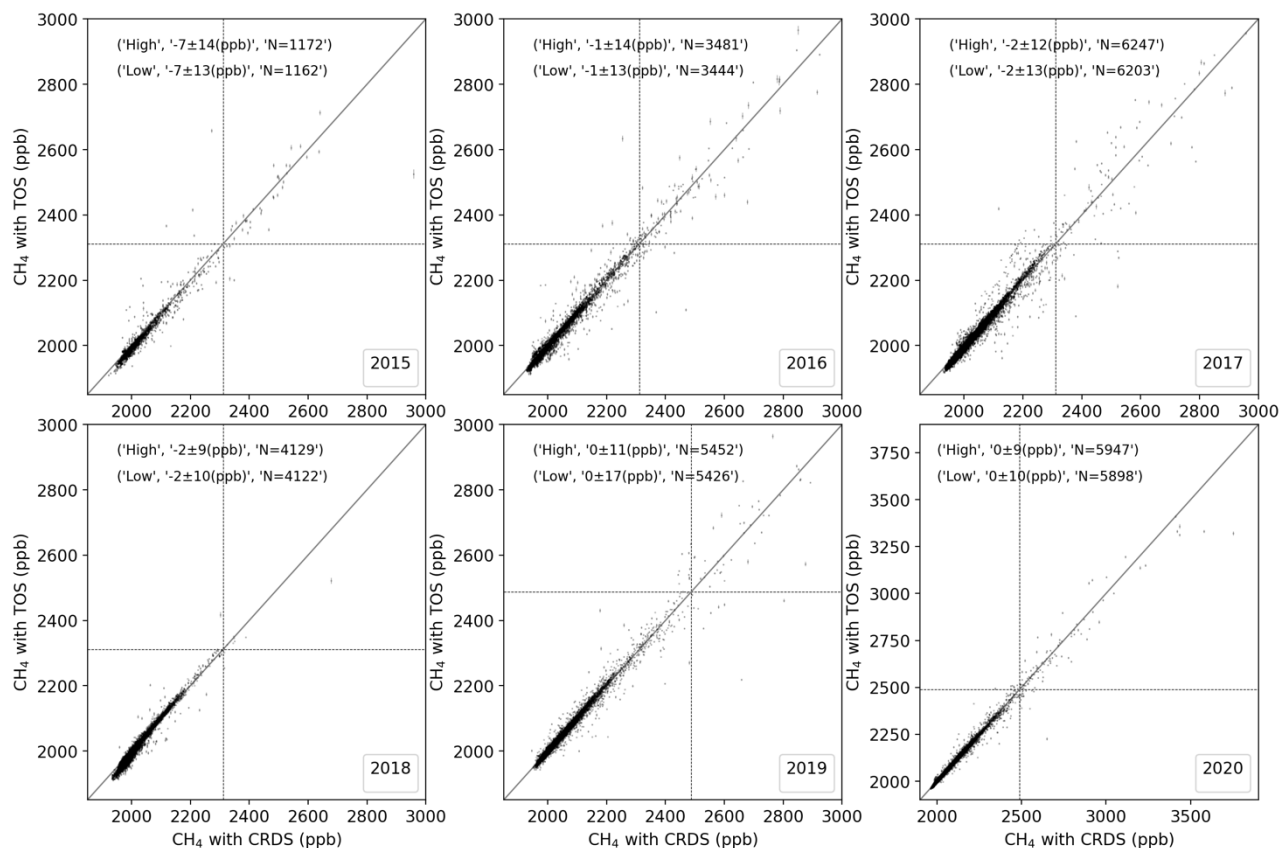


Figure 7. Relationship between CH₄ concentration measured by the TOS and the CRDS during ambient air measurements at KRS. The CRDS 3-minute measurements are averaged on the horizontal axis, and the TOS values are on the vertical axis. Error bars on the horizontal axis are the standard deviation of the averaged data. Error bars on the vertical axis are U_{x_sample} . The gray line represents the 1:1 line. The dotted lines indicate the highest concentration of standard gases. The average difference between TOS and CRDS (TOS – CRDS) for each inlet is represented in the figure (mean ± SD). Only data that were within the standard gas concentration range were used.

Data availability

335 The data are available from the Global Environmental Database, hosted by GED, CGER, NIES (<http://db.cger.nies.go.jp/portal/geds/index>).

Author contribution

MS and NT designed the study. MS wrote the manuscript. MA, DD, and AF conducted the measurements. All authors contributed to the discussion and preparation of the manuscript.



340 **Competing interests**

The authors declare that they have no conflict of interest.

Acknowledgments

We thank Sergey Mitin (Institute of Microbiology, Russian Academy of Sciences) for administrative support. Our research was financially supported by the Global Environmental Research Coordination System from Ministry of the Environment of
345 Japan and the most important innovative project of national importance "Development of a system for ground-based and remote monitoring of carbon pools and greenhouse gas fluxes in the territory of the Russian Federation, ensuring the creation of recording data systems on the fluxes of climate-active substances and the carbon budget in forests and other terrestrial ecological systems" (Registration number: 123030300031-6).

References

- 350 Andrews, A. E., Kofler, J. D., Trudeau, M. E., Williams, J. C., Neff, D. H., Masarie, K. A., Chao, D. Y., Kitzis, D. R., Novelli, P. C., Zhao, C. L., Dlugokencky, E. J., Lang, P. M., Crotwell, M. J., Fischer, M. L., Parker, M. J., Lee, J. T., Baumann, D. D., Desai, A. R., Stanier, C. O., De Wekker, S. F. J., Wolfe, D. E., Munger, J. W., and Tans, P. P.: CO₂, CO, and CH₄ measurements from tall towers in the NOAA Earth System Research Laboratory's Global Greenhouse Gas Reference Network: instrumentation, uncertainty analysis, and recommendations for future high-accuracy greenhouse gas monitoring efforts,
355 Atmospheric Measurement Techniques, 7, 647-687, 10.5194/amt-7-647-2014, 2014.
- ICOS RI: ICOS Atmosphere Station Specifications V2.0, edited by: Laurent, O., ICOS ERIC, <https://doi.org/10.18160/GK28-2188>, 2020.
- Kwok, C. Y., Laurent, O., Guemri, A., Philippon, C., Wastine, B., Rella, C. W., Vuillemin, C., Truong, F., Delmotte, M., Kazan, V., Darding, M., Lebegue, B., Kaiser, C., Xueref-Remy, I., and Ramonet, M.: Comprehensive laboratory and field
360 testing of cavity ring-down spectroscopy analyzers measuring H₂O, CO₂, CH₄ and CO, Atmospheric Measurement Techniques, 8, 3867-3892, 10.5194/amt-8-3867-2015, 2015.
- Machida, T., Tohjima, Y., Katsumata, K. and Mukai, H.: A new CO₂ calibration scale based on gravimetric one-step dilution cylinders in National Institute for Environmental Studies – NIES 09 CO₂ Scale, in Report of the 15th WMO/IAEA Meeting of Experts on Carbon Dioxide, Other Greenhouse Gases and Related Tracers Measurement Techniques (ed. Willi A. Brand). Jena,
365 Germany, September 7–10, 2009, WMO/GAW Report No. 194, 165–169, 2011.
- Sasakawa, M., Machida, T., Tsuda, N., Arshinov, M., Davydov, D., Fofonov, A., and Krasnov, O.: Aircraft and tower measurements of CO₂ concentration in the planetary boundary layer and the lower free troposphere over southern taiga in West Siberia: Long-term records from 2002 to 2011, Journal of Geophysical Research-Atmospheres, 118, 9489-9498, 10.1002/jgrd.50755, 2013.



- 370 Sasakawa, M., Ito, A., Machida, T., Tsuda, N., Niwa, Y., Davydov, D., Fofonov, A., and Arshinov, M.: Annual variation of CH₄ emissions from the middle taiga in West Siberian Lowland (2005-2009): a case of high CH₄ flux and precipitation rate in the summer of 2007, *Tellus Series B-Chemical and Physical Meteorology*, 64, ARTN 17514 10.3402/tellusb.v64i0.17514, 2012.
- Sasakawa, M., Shimoyama, K., Machida, T., Tsuda, N., Suto, H., Arshinov, M., Davydov, D., Fofonov, A., Krasnov, O., Saeki,
375 T., Koyama, Y., and Maksyutov, S.: Continuous measurements of methane from a tower network over Siberia, *Tellus Series B-Chemical and Physical Meteorology*, 62, 403-416, 10.1111/j.1600-0889.2010.00494.x, 2010.
- Suto, H. and Inoue, G.: A New Portable Instrument for In Situ Measurement of Atmospheric Methane Mole Fraction by Applying an Improved Tin Dioxide-Based Gas Sensor, *J Atmos Ocean Tech*, 27, 1175-1184, 10.1175/2010jtecha1400.1, 2010.
- Watai, T., Machida, T., Shimoyama, K., Krasnov, O., Yamamoto, M., and Inoue, G.: Development of an Atmospheric Carbon
380 Dioxide Standard Gas Saving System and Its Application to a Measurement at a Site in the West Siberian Forest, *J Atmos Ocean Tech*, 27, 843-855, 10.1175/2009jtecha1265.1, 2010.
- WMO: 19th WMO/IAEA Meeting on Carbon Dioxide, Other Greenhouse Gases and Related Tracers Measurement Techniques (GGMT-2017), Dübendorf, Switzerland, 27–31 August 2017, GAW Report No. 242, World Meteorological Organization, Geneva, Switzerland, 2018.

385